Non-Binary LDPC Code Optimization for Partial-Response Channels

Ahmed Hareedy[1], Behzad Amiri[1], Shancheng Zhao[1], Richard Galbraith[2], and Lara Dolecek[1]
[1]Electrical Eng. Department, University of California, Los Angeles, Los Angeles, CA 90095 USA
[2]Hitachi Global Storage Technologies, A Western Digital Company, Rochester, MN 55901 USA
{ahareedy, amiri}@ucla.edu, zhaoday@mail2.sysu.edu.cn, rick.galbraith@hgst.com, and dolecek@ee.ucla.edu

***Abstract*—In this paper, we analyze and optimize non-binary low-density parity-check (NB-LDPC) codes for magnetic recording applications. While the topic of the error floor performance of binary LDPC codes over additive white Gaussian noise (AWGN) channels has recently received considerable attention, very little is known about the error floor performance of NB-LDPC codes over other types of channels, despite the early results demonstrating superior characteristics of NB-LDPC codes relative to their binary counterparts. We first show that, due to outer looping between detector and decoder in the receiver, the error profile of NB-LDPC codes over partial-response (PR) channels is qualitatively different from the error profile over AWGN channels – this observation motivates us to introduce new combinatorial definitions aimed at capturing decoding errors that dominate PR channel error floor region. We call these errors (or objects) balanced absorbing sets (BASs), which are viewed as a special subclass of previously introduced absorbing sets (ASs). Additionally, we prove that due to the more restrictive definition of BASs (relative to the more general class of ASs), an additional degree of freedom can be exploited in code design for PR channels. We then demonstrate that the proposed code optimization aimed at removing dominant BASs offers improvements in the frame error rate (FER) in the error floor region by up to 2.5 orders of magnitude over the uninformed designs. Our code optimization technique carefully yet provably removes BASs from the code while preserving its overall structure (node degree, quasi-cyclic property, regularity, etc.). The resulting codes outperform existing binary and NB-LDPC solutions for PR channels by about 2.5 and 1.5 orders of magnitude, respectively.**

I. Introduction

Practical 1-D magnetic-recording (MR) channels are usually modeled as partial-response (PR) channels [1]. Signal processing techniques for PR channels focus on detection and channel coding methods. Detection methods based on the turbo principles have been thoroughly investigated, e.g., [2] and [3]. Since MR applications must run at very low bit error rates, LDPC codes have already been studied in the context of PR channel; [3] and [4] have investigated binary LDPC codes and their error floors in this context. While it has long been known that non-binary LDPC (NB-LDPC) codes outperform their binary counterparts [5], not much work has been done on NB-LDPC codes for PR channels. First results on this topic include [6] – [8]. Work in [6] investigated the progressive-edge-growth (PEG) algorithm to design NB-LDPC codes for PR channels, and the works in [7] and [8] studied non-binary quasi-cyclic LDPC (NB-QC-LDPC) codes for PR channels.

In this work, we offer a complete study of the PR channel error floor performance of structured and regular NB-LDPC codes and provide design guidelines to optimize these codes for PR channels. In particular, we show that the error profile in the error floor region over PR channels is different from the one over additive white Gaussian noise (AWGN) channels. A subset of absorbing sets (ASs) [9], called balanced absorbing sets (BASs), is introduced and is shown to be the dominant error type over PR channels. By focusing on the removal of this special subclass of ASs from the Tanner graph of an NB-LDPC code, we are able to eliminate all detrimental configurations while preserving code structure.

Additionally, we suitably modify the algorithm initially proposed in [10] to now offer NB-LDPC codes with superior error floor performance over PR channels. Our simulation results show that our optimized codes have up to 2.5 (or 1.5 at half the latency) orders of magnitude error floor performance improvement compared to the unoptimized ones. Furthermore, the NB-LDPC codes optimized using our algorithm outperform previously proposed LDPC codes in [3], [7], and [8].

In Section II, the system model is presented. Section III, aided by some new theoretical definitions, describes the error structures contributing to the error floor over PR channels. Further discussion on the BASs and the techniques to remove them are presented in Section IV. The code design is presented in Section V along with the improved optimization algorithm and simulation results. The paper is concluded in Section VI.

II. System Model

In this section, we introduce the system model for NB-LDPC coded PR channel which will be used throughout this paper. Consider an NB-LDPC code over GF(q), $q = 2^m$, with block length L and dimension K. The system model, shown in Fig. 1, has the following components:

Encoding: The information sequence $\underline{u} = (u_0, u_1, \ldots, u_{K-1}) \in \text{GF}(q)^K$ is encoded into a codeword $\underline{v} = (v_0, v_1, \ldots, v_{L-1}) \in \text{GF}(q)^L$. In this paper, we focus on NB-QC-LDPC codes e.g., [10] and [11], which are known to have good performance as well as implementation-friendly structure.

Transmission: The codeword $\underline{v}$ is converted to the binary sequence $\underline{d} = (d_0, d_1, \ldots, d_{N-1})$ with $N = mL$. Then, $\underline{d}$ is interleaved psuedo-randomly and written onto a PR channel.

Channel: The 1-D MR channel includes inter-symbol interference (ISI) in addition to jitter and electronic noise. The normalized MR channel density is 1.4 (see also [12]). The MR channel output is the oversampled sequence denoted by $\underline{x}$.

Reception: Continuous-time filtering (CTF) and down-sampling are applied sequentially to the sequence $\underline{x}$. The resulting sequence is passed through a digital finite impulse response (DFIR) filter. CTF and DFIR units are used to achieve the PR equalization target (the used target is [8 14 2]).

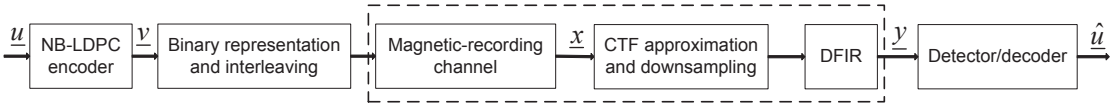

Fig. 1. System model for 1-D MR channel utilizing an NB-LDPC code.

Detection/Decoding: A finite-precision fast Fourier transform based q-ary sum-product algorithm (FFT-QSPA) LDPC decoder [13] and a BCJR detector, which is based on pattern-dependent noise prediction (PDNP), are used to iteratively recover the original information sequence $\underline{u}$.

The iterations executed internally inside the LDPC decoder are referred to as **local iterations**. Each outer looping between the detector and the decoder is referred to as one **global iteration**. In between two consecutive global iterations, the decoder executes its prescribed number of local iterations (or fewer, if a codeword is reached).

III. Error Profile of NB-LDPC Codes over PR Channels

A. A Motivating Example

We use the following example to illustrate that the error profiles for PR and AWGN channels are qualitatively different; we observed similar behavior for other channel and code parameters. We define e_w as the error weight.

Example 1. *Consider an NB-QC-LDPC code with a block length $N = 4092$ bits, rate $R \approx 0.87$, $q = 16$, and column weight $c = 4$. Fig. 2 shows the performance plots of this code over PR and AWGN channels. Tables I and II show the error profiles at representative SNR values. The tables show that the dominant error in case of PR channel is the $(6, 2)$ AS while the dominant errors in case of AWGN channel are the $(4, 4)$, $(6, 4)$, and $(6, 6)$ ASs. (BAS in Table I refers to balanced absorbing set, which we will introduce shortly.)*

Our extensive simulations for different column weights confirm that indeed the PR channel error profile is different from the AWGN channel error profile; for example, for column weight $c = 3$, the dominant error in case of PR channel is the $(6, 0)$ AS while it is the $(3, 3)$ AS in case of AWGN channel.

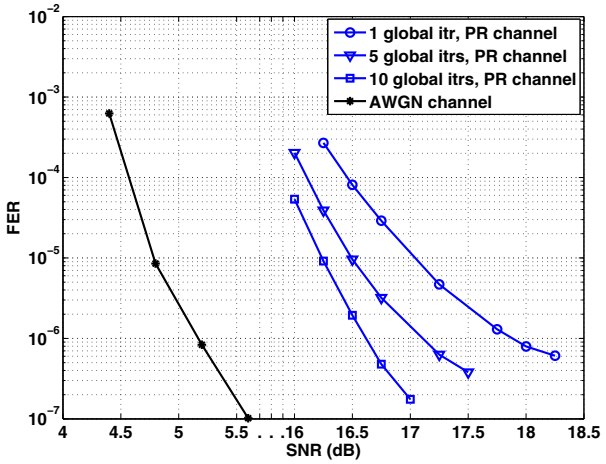

Fig. 2. FER curves over PR and AWGN channels for the NB-QC-LDPC code, $N = 4092$ bits, $R \approx 0.87$, $q = 16$, and $c = 4$.

TABLE I
Error profile for the PR channel performance curves shown in Fig. 2 for 10 global iterations, SNR = 16.75 dB, FER = 4.79E−7.

Error Weight	Low ($e_w < 4$)	Medium ($4 \le e_w < 12$)				High ($e_w \ge 12$)	
Type	0	BAS $(6, 2)$	BAS other	UBAS	Random	BAS Comb.	Random
Count		86	5	2	2	4	1

TABLE II
Error profile for the AWGN channel performance curves shown in Fig. 2, SNR = 5.60 dB, FER = 1.05E−7.

Error Type	$(4, 4)$	$(5, 2)$	$(6, 2)$	$(6, 4)$	$(6, 6)$	$(7, 5)$	Other
Count	52	5	8	19	14	4	15

B. New Definitions of Structured Errors

Motivated by the AWGN and PR channels error profile differences shown in the last subsection, we now introduce new combinatorial definitions aimed at capturing the decoding errors under PR channel. The definition of AS is recalled first.

Definition 1. (cf. [9]) *Consider a subgraph induced by a subset $\mathcal{V}$ of variable nodes in the bipartite graph of the code. The set $\mathcal{V}$ is said to be an (a, b) **absorbing set (AS)** if the size of $\mathcal{V}$ is a, the number of neighboring unsatisfied check nodes is b and each variable node in $\mathcal{V}$ is connected to strictly more satisfied than unsatisfied neighboring check nodes.*

Definition 2. (cf. [14]) *An **elementary absorbing set** is an absorbing set with each of its neighboring satisfied checks having two edges connected to it, and each of its neighboring unsatisfied checks having exactly one edge connected to it.*

Remark 1. (cf. [10]) *For a **non-binary elementary absorbing set**, the unlabeled subgraph is a binary AS, and all the cycles of this subgraph satisfy the following weight equation:*

$$\prod_{i=1}^{t} w_{2i-1} = \prod_{i=1}^{t} w_{2i} \text{ over GF}(q), \tag{1}$$

*where w_j's, $1 \le j \le 2t$, are edge weights and $2t$ is the length of the cycle. Note that for a non-binary AS which is **not elementary**, the equation (1) does not necessarily hold for all of its cycles.*

Let $g = \left\lfloor \frac{c-1}{2} \right\rfloor$ for a given column weight c. Aided by the simulation results of the type shown in Example 1, we classify ASs as follows, depending on the relative value of b.

Definition 3. *An absorbing set that has $0 \le b \le \left\lfloor \frac{ag}{2} \right\rfloor$ is defined as a **balanced absorbing set (BAS)**.*

Definition 4. *An absorbing set that has $\left\lfloor \frac{ag}{2} \right\rfloor < b \le ag$ is defined as an **unbalanced absorbing set (UBAS)**.*

BASs play a critical role in the error profile of PR channels.

Examples of BASs include $(6,0)$ AS for $c=3$ ($g=1$), and $(8,3)$ and $(6,2)$ ASs for $c=4$ ($g=1$). Codewords are special cases of BASs ($b=0$). Examples of UBASs include $(3,3)$ AS for $c=3$, and $(6,4)$ and $(6,6)$ ASs for $c=4$.

C. Effect of Global Iterations

In addition to having an error profile different from the AWGN channel case, we further observe that in the PR channel case, the error profile changes as a function of the number of global iterations. For the code in Example 1, Fig. 2 shows the performance plots over PR channel at 1, 5, and 10 global iterations. This example serves to illustrate the error profile spectra; we have observed a similar behavior for other codes and system parameters. For this example, we tabulate the errors in Tables III, IV, and I for 1, 5, and 10 global iterations, respectively. Observe that, when the receiver executes a relatively low number of global iterations (say e.g., 5), the decoding errors are usually due to BASs and their combinations. In fact, through our extensive simulations (not reported due to space limitations), we observed that high weight errors are mostly combinations of a special class of BASs, which are of low weight. This observation motivates the following definition.

Let s be the weight of the smallest dominant BAS in the error floor region for PR channel (for a sufficient number of global iterations).

Definition 5. *A balanced absorbing set that has $s \leq a < 2s$ is defined as a **first-order balanced absorbing set (FOBAS)**.*

A high weight error can thus be succinctly expressed as a combination of multiple FOBASs.

TABLE III
ERROR PROFILE FOR THE PR CHANNEL PERFORMANCE CURVES SHOWN IN FIG. 2 FOR 1 GLOBAL ITERATION, SNR = 18.00 DB, FER = 7.96E−7.

Error Weight	Low ($e_w < 4$)	Medium ($4 \leq e_w < 12$)			High ($e_w \geq 12$)	
Type	15	BAS	UBAS	Random	BAS Comb.	Random
Count		0	13	27	13	32

TABLE IV
ERROR PROFILE FOR THE PR CHANNEL PERFORMANCE CURVES SHOWN IN FIG. 2 FOR 5 GLOBAL ITERATIONS, SNR = 17.25 DB, FER = 6.3E−7.

Error Weight	Low ($e_w < 4$)	Medium ($4 \leq e_w < 12$)				High ($e_w \geq 12$)	
Type	0	BAS $(6,2)$	BAS other	UBAS	Random	BAS Comb.	Random
Count		47	5	5	11	23	9

The errors in Tables III, IV, and I are classified into:

1) Low weight errors: Such errors are of weight less than the minimum AS size (a_{min}). These errors occur due to the intrinsic memory of PR channel, and are typically prevented by the CTF and DFIR units. Increasing the number of global iterations is generally sufficient to eliminate these decoding errors (as shown in the tables).
2) Medium weight errors: These decoding errors have weight e_w such that $a_{min} \leq e_w < 2s$. In Example 1, $s=6$ and $a_{min}=4$ (because $c=4$ [10]) and thus, medium weight errors have $4 \leq e_w < 12$. The tables reveal that as the number of global iterations increases, medium weight errors dominate the error profile and they are overwhelmingly BASs.
3) High weight errors: These decoding errors have weight $e_w \geq 2s$. As the number of global iterations increases, these errors are mostly resolved. Also, they are typically combinations of FOBASs.

Intuitively, the increase in the number of global iterations provides sufficient innovation at the decoder input to resolve AS errors that are on the brink of instability, which we classified as UBASs. As a result, the remaining, unresolved errors are due to BASs. Additionally, due to the memory in the PR channel system, a wrong belief at a variable node negatively impacts nodes that are adjacent to it. With a sufficient number of variable nodes having wrong beliefs, a BAS decoding error occurs. With the memory in the system, these errors propagate to adjacent variable nodes that themselves form another BAS. As a result, high weight errors containing several small BASs (which we refer to as FOBASs) are observed.

Remark 2. *The increase in the number of global iterations resolves the majority of high weight errors (see e.g., Table I); however, solely relying on the increase in the number of global iterations is not a preferred strategy in practice because of the added decoding latency. In our code design approach, we will therefore focus on removing FOBASs (and consequently their combinations).*

IV. ANALYZING BALANCED ABSORBING SETS

Our goal is to provably eliminate detrimental objects from the Tanner graph of an NB-QC-LDPC code, which we have identified to be FOBASs for PR channel. Our removal process will carefully modify edge weights in the Tanner graph so that the resultant code is free of FOBASs. In order to perform this process, we first establish some properties of BASs/FOBASs to be removed (Section IV-A), and then discuss the operations on the edge weights that need to be performed in order to remove an object of interest (Section IV-B).

A. Preparing the List of Problematic Objects

Let us first establish some properties of BASs and FOBASs.

Lemma 1. *For a given a, the total number of (a,b) pairs that can result in a BAS is given by:*

$$M_{BAS}|_a = \left\lfloor \frac{ag}{2} \right\rfloor + 1, \tag{2}$$

while for a given s, the total number of (a,b) pairs that can result in an FOBAS is approximately:

$$M_{FOBAS}|_s \approx \frac{3s^2 g}{4}. \tag{3}$$

Proof. The proof of (2) follows from Definition 3 of BAS:

$$M_{BAS}|_a = \sum_{b=0}^{\left\lfloor \frac{ag}{2} \right\rfloor} 1 = \left\lfloor \frac{ag}{2} \right\rfloor + 1.$$

To obtain (3), we first consider the case when both g and s are even. Recalling the definition of FOBAS (Definition 5) and combining that with (2) gives:

$$M_{FOBAS}|_s = \sum_{a=s}^{2s-1} \left(\frac{ag}{2}+1\right) = \left(\frac{sg}{2}+1\right) + \left(\frac{(s+1)\,g}{2}+1\right) + \left(\frac{(s+2)\,g}{2}+1\right) + \cdots + \left(\frac{(2s-1)\,g}{2}+1\right) = \frac{3s^2g}{4} + \left(1-\frac{1}{4}g\right)s \approx \frac{3s^2g}{4}.$$

The same procedure can be followed for other choices of the values of g and s. For example, if $g=1$ and s is even, $M_{FOBAS}|_s = \frac{3s^2}{4} + \frac{s}{2}$. It can be shown that the dominant term, $\frac{3s^2g}{4}$, remains the same in all cases. □

Example 2. *Consider the NB-QC-LDPC code in Example 1 where $s=6$ and $g = \left\lfloor \frac{c-1}{2} \right\rfloor = 1$. In this example, the total number of $(6,b)$ pairs*[1] *that can result in a BAS is $M_{BAS}|_{a=6} = 4$. The total number of (a,b) pairs*[2] *that can result in an FOBAS is $M_{FOBAS}|_{s=6} = 30$.*

Remark 3. *Lemma 1 provides the count of the (a,b) candidate pairs which are problematic for PR channels. If there are multiple non-isomorphic configurations with the same values of (a,b), they should all be accounted for during the code optimization process. Nonetheless, Lemma 1 provides a first-order characterization of BASs and FOBASs.*

Remark 4. *Ensemble-wide counting of the number of (a,b) binary elementary ASs is done in [14] and, for a given (a,b) binary elementary AS, the fraction of edge weights that can result in a non-binary elementary AS is given in [10].*

B. Removing Balanced Absorbing Sets

Since our focus in the PR channel system is on the restricted subclass of ASs, given by BASs, it is sufficient to eliminate only this special class of objects. The object removal can be performed by changing only the edge weights, i.e., without altering the underlying topology of the Tanner graph. This is a particularly desirable feature as it maintains the underlying implementation-friendly code structure and properties. Thus, we can preserve the code structure while improving its performance. Restricting the object removal process to only the class of BASs offers an additional degree of freedom, compared to the case of removing the more general class of ASs, as would for example be necessary in the AWGN channel system (see [10]). We capture this difference in the following lemma.

Lemma 2. *The minimum number of edge weights to be changed to remove an (a,b) AS is given by:*

$$E_{AS,min} = (g - b_{vn,max} + 1)\,, \tag{4}$$

where $b_{vn,max}$ is the maximum number of unsatisfied check nodes per variable node in the subgraph of this object, while the minimum number of edge weights to be changed to remove an (a,b) BAS is given by:

$$E_{BAS,min} = min\left\{E_{AS,min}, \left(\left\lfloor \frac{ag}{2} \right\rfloor - b + 1\right)\right\}. \tag{5}$$

Proof. To remove an AS, this configuration needs to be converted into a non-AS. It suffices to increase the number of unsatisfied check nodes to be (just) above $\left\lfloor \frac{c-1}{2} \right\rfloor$ for any given variable node in the configuration. The number of necessary edge weight changes is then clearly minimized if we choose the variable node that has the highest number of unsatisfied check nodes, denoted by $b_{vn,max}$, to begin with. Thus,

$$E_{AS,min} = \left\lfloor \frac{c-1}{2} \right\rfloor - b_{vn,max} + 1 = g - b_{vn,max} + 1,$$

where the last equality comes from the definition of g.

On the other hand, to remove a BAS, we may not only convert it into a non-AS (as before), but also we may convert it into a UBAS. (As we shall see later, this choice offers greater flexibility in the edge weight selection.)

To convert a BAS into a UBAS, it suffices to increase b to be (just) above $\left\lfloor \frac{ag}{2} \right\rfloor$. Thus, the minimum number of edge weights to be changed will be:

$$E_{BU,min} = b_{new} - b = \left\lfloor \frac{ag}{2} \right\rfloor - b + 1. \tag{6}$$

Computing the minimum of (4) and (6) gives us the minimum number of edge weights to be changed to remove a BAS. □

We illustrate the lemma with the following example.

Example 3. *Fig. 3 shows a $(4,2)$ BAS where $c=3$ ($g=1$). Thus, $a=4$, $b=2$, and $b_{vn,max}=1$. Equations* (4) *and* (6) *from Lemma 2 give $E_{AS,min} = E_{BU,min} = 1$, which means $E_{BAS,min} = 1$. This indicates that the problematic object can be removed by changing only 1 edge weight. From Fig. 3, there are $\binom{10}{1}$ selections to remove the BAS (make it a non-AS or a $(4,3)$ UBAS), while there are only $\binom{8}{1}$ selections to convert this structure to a non-AS because the edges connected to c_5 do not count in this case (changing their weights converts the structure into a UBAS which is still an AS).*

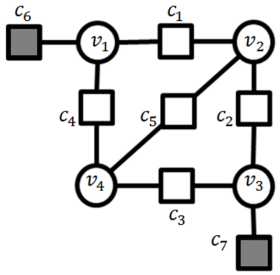

Fig. 3. $(4,2)$ balanced absorbing set and $c=3$.

V. Code Optimization for Transmission over PR Channel

A. The Improved Optimization Algorithm

We are now ready to state our code optimization algorithm. Our algorithm is inspired by the algorithm in [10] (which we will refer to as the baseline algorithm), with the following PR channel-specific refinements:

[1]These pairs are $(6,0)$, $(6,1)$, $(6,2)$, and $(6,3)$.

[2]These pairs are $(6,0)$, $(6,1)$, …, $(6,3)$, $(7,0)$, $(7,1)$, …, $(7,3)$, …, $(11,0)$, $(11,1)$, …, $(11,5)$.

Algorithm 1 Design of NB-QC-LDPC codes with reduced number of problematic objects

Input: Tanner graph G with edge weights over GF(q).
Determine W, the set of BASs to be eliminated, and F, the set of all FOBAS candidate (a, b) pairs given s.
Let X be the set of BASs that can not be eliminated and initialize it with $\emptyset$.
Let A be the set of BASs in W that have been processed and initialize it with $\emptyset$.
Find the smallest BAS (a_j, b_j) in $W \backslash A$.
Find Z_j, the set of all (a_j, b_j) BASs in the unlabeled version of the Tanner graph G.
for $\forall z \in Z_j$ **do**
  Determine $\mathcal{E}_z$, the set of all edges in z.
  if the weights of edges in $\mathcal{E}_z$ are such that the configuration is a BAS **then**
    For an edge $k \in \mathcal{E}_z$, check the weight $w_k^{'}$ where $w_k^{'} \neq w_k$ and $w_k^{'} \neq 0$.
    if the configuration changes to a non-AS or to an AS with $b > \lfloor \frac{ag}{2} \rfloor$, which is a UBAS having (a, b) pair $\notin F$, **then**
      Replace w_k with $w_k^{'}$.
    else
      $\mathcal{E}_z \leftarrow \mathcal{E}_z \backslash k$.
      if $\mathcal{E}_z = \emptyset$ **then**
        $X \leftarrow X \cup Z_j$ and go to 23.
      else
        Go to 10.
      end if
    end if
  end if
end for
Add (a_j, b_j) BAS to the set A.
If $A \neq W$, go to 5.
If $X = \emptyset$, all BASs of interest are eliminated. Otherwise, it is not possible to eliminate BASs in X.

1) The list of problematic objects to remove is channel dependent; in the PR channel case, it suffices to focus only on the class of BASs.
2) Since only BASs, as a certain subclass of ASs, have to be removed in the PR channel case, we now have a greater flexibility in choosing appropriate edge weights, which in turn enables us to remove all detrimental objects.

B. Simulation Results

In this subsection, we report simulation results for various NB-QC-LDPC codes, optimized using our proposed method.

Code 1 is an NB-QC-LDPC code defined over GF(4), with $N \approx 870$ bits, $R \approx 0.82$, and $c = 3$. This code is optimized for PR channel by removing the FOBASs $(6, 0)$, $(6, 1)$, $(8, 0)$, $(8, 4)$, and $(10, 0)$ using Algorithm 1. Code 2 is an NB-QC-LDPC code defined over GF(16), with $N = 4092$ bits, $R \approx 0.87$, and $c = 4$. This code is derived from the code presented in Example 1 after being optimized for PR channel by removing the FOBASs $(6, 2)$, $(6, 3)$, and $(8, 2)$ using Algorithm 1. Finally, Code 3 is an NB-QC-LDPC code defined over GF(4), with $N = 1058$ bits, $R \approx 0.87$, and $c = 3$. Code 3 is optimized for PR channel by removing the same objects as Code 1. All the unoptimized codes are high-performance codes that are generated according to [11].

Figures 4 and 5 show the simulation results for Codes 1 and 2, respectively. The error floor performance of these optimized codes is improved by 2 orders of magnitude in Fig. 4 and 2.5 orders of magnitude in Fig. 5 compared to the unoptimized ones. In both figures, the optimized codes at 5 global iterations outperform the unoptimized ones at 10 global iterations by nearly 1.5 orders of magnitude. Thus, our optimized codes enjoy better performance at reduced latency. Tables V, VI, VII, and VIII confirm the reduction in numbers of BASs and BAS combinations in the error profile over PR channel of these optimized codes. For example, for Code 2, comparing Table VIII with Table I demonstrates the elimination of BAS errors (from 91 to 0) while comparing Table VII with Table IV demonstrates the elimination of both BAS errors (from 52 to 0) and most BAS combinations errors (from 23 to 3).

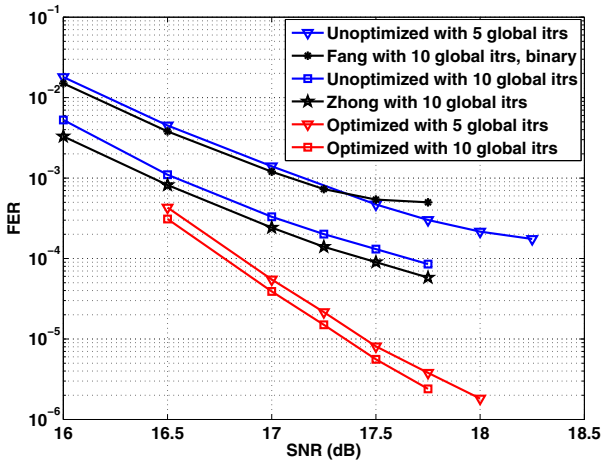

Fig. 4. FER curves over PR channel for the unoptimized and optimized NB-QC-LDPC codes, $N \approx 870$ bits, $R \approx 0.82$, $q = 4$, and $c = 3$.

TABLE V
ERROR PROFILE FOR THE OPTIMIZED PERFORMANCE CURVES SHOWN IN FIG. 4 AT 5 GLOBAL ITERATIONS, SNR = 18.00 DB, FER = 1.82E−6.

Error Weight	Low ($e_w < 3$)	Medium ($3 \leq e_w < 12$)				High ($e_w \geq 12$)	
Type	0	BAS $(6, 0)$	BAS other	UBAS	Random	BAS Comb.	Random
Count		0	0	4	9	4	13

TABLE VI
ERROR PROFILE FOR THE OPTIMIZED PERFORMANCE CURVES SHOWN IN FIG. 4 AT 10 GLOBAL ITERATIONS, SNR = 17.50 DB, FER = 5.59E−6.

Error Weight	Low ($e_w < 3$)	Medium ($3 \leq e_w < 12$)				High ($e_w \geq 12$)	
Type	0	BAS $(6, 0)$	BAS other	UBAS	Random	BAS Comb.	Random
Count		0	0	3	10	2	15

Fig. 4 also presents the performance of previously proposed codes for PR channels. In particular, our proposed code outperforms the binary LDPC code in [3] (labeled Fang) by more than 2 orders of magnitude and the NB-LDPC code in [7] and [8] (labeled Zhong) by more than 1 order of magnitude, and it does so at half of the decoding latency.

Additionally, we demonstrate the need to focus on the error events that are specific to PR channel when designing codes

for such channels. The black curve in Fig. 5 presents the PR channel performance of the code in Example 1 after being optimized for AWGN channel (by removing $(4,4)$, $(6,4)$, and $(6,6)$ UBASs, see also Example 1). It is clear that naively using a code optimized for the AWGN channel will not work as well for the PR channel since the combinatorial properties of the decoding errors for the two channels are different.

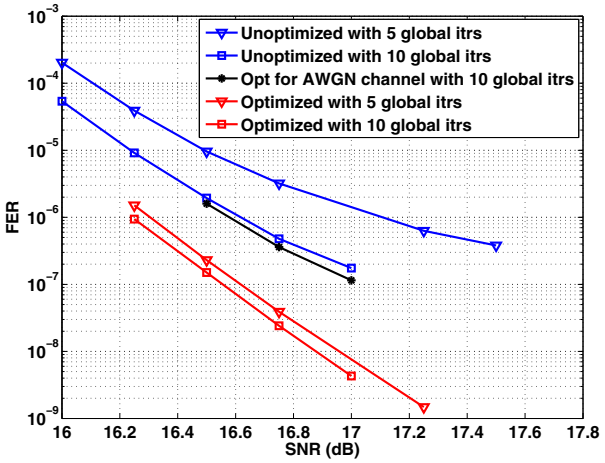

Fig. 5. FER curves over PR channel for the unoptimized and optimized NB-QC-LDPC codes, $N = 4092$ bits, $R \approx 0.87$, $q = 16$, and $c = 4$.

TABLE VII
ERROR PROFILE FOR THE OPTIMIZED PERFORMANCE CURVES SHOWN IN FIG. 5 AT 5 GLOBAL ITERATIONS, SNR = 17.25 DB, FER = 1.48E−9.

Error Weight	Low ($e_w < 4$)	Medium ($4 \le e_w < 12$)				High ($e_w \ge 12$)	
Type	0	BAS $(6,2)$	BAS other	UBAS	Random	BAS Comb.	Random
Count		0	0	5	8	3	14

TABLE VIII
ERROR PROFILE FOR THE OPTIMIZED PERFORMANCE CURVES SHOWN IN FIG. 5 AT 10 GLOBAL ITERATIONS, SNR = 16.75 DB, FER = 2.41E−8.

Error Weight	Low ($e_w < 4$)	Medium ($4 \le e_w < 12$)				High ($e_w \ge 12$)	
Type	0	BAS $(6,2)$	BAS other	UBAS	Random	BAS Comb.	Random
Count		0	0	2	9	2	17

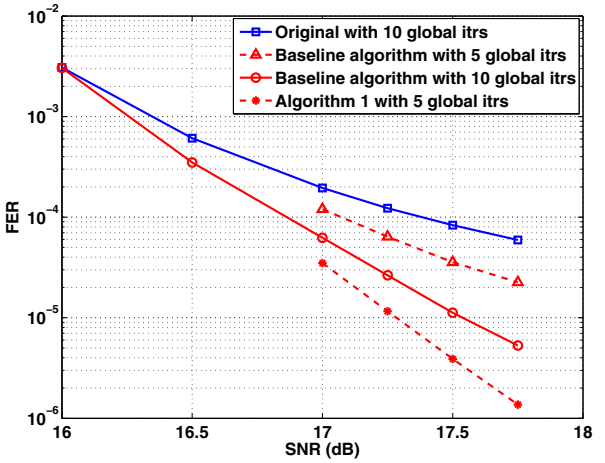

Fig. 6. FER curves over PR channel for the NB-QC-LDPC codes optimized using the baseline algorithm and Algorithm 1, $N = 1058$ bits, $R \approx 0.87$, $q = 4$, and $c = 3$.

Lastly, Fig. 6 shows the benefits of Algorithm 1 over the baseline algorithm, when applied in the context of PR channel. Code 3, which is optimized using Algorithm 1, at 5 global iterations outperforms the code which is optimized using the baseline algorithm at 10 global iterations by about 0.5 order of magnitude. The performance improvement is mainly due to the additional degree of freedom provided by targeting BASs (and not the larger class of ASs), which makes it more likely that appropriate edge weight choices can be made during the object removal process (see also Lemma 2 and Example 3).

VI. CONCLUSION

In this work, we studied in detail the error floor performance of NB-QC-LDPC codes over PR channels. We demonstrated that the error profile over PR channel is different than that over AWGN channel; the existing code optimization techniques previously developed for the AWGN channel transmission are thus not effective. We introduced a restricted class of combinatorial objects, called balanced absorbing sets (BASs), that were identified to be the key contributor to the PR channel error floor. We proposed an algorithm for code design provably free of detrimental BASs. Simulation results demonstrated that the proposed codes outperform existing constructions by more than an order of magnitude at half the decoding latency.

ACKNOWLEDGEMENT

The research was supported by NSF and an IDEMA-ASTC grant.

REFERENCES

[1] B. Vasic and E. Kurtas, *Coding and signal processing for magnetic recording systems.* CRC Press, 2005.

[2] G. Colavolpe and G. Germi, "On the application of factor graphs and the sum-product algorithm to ISI channels," *IEEE Trans. Commun.*, vol. 53, no. 5, pp. 818 - 825, May 2005.

[3] Y. Fang, P. Chen, L. Wang, and F. Lau, "Design of protograph LDPC codes for partial response channels," *IEEE Trans. Commun.*, vol. 60, no. 10, pp. 2809 - 2819, Oct. 2012.

[4] Y. Han and W. Ryan, "Low-floor detection/decoding of LDPC-coded partial response channels," *IEEE Jour. Sel. Areas Commun.*, vol. 28, no. 2, pp. 252 - 260 , Feb. 2010.

[5] M. Davey and D. MacKay, "Low-density parity-check codes over GF(q)," *IEEE Commun. Lett.*, vol. 2, no. 6, pp. 165 - 167, June 1998.

[6] S. Jeon and B. Kumar, "Binary SOVA and nonbinary LDPC codes for turbo equalization in magnetic recording channels," *IEEE Trans. Magn.*, vol. 46, no. 6, pp. 2248 - 2251, June 2010.

[7] H. Zhong, T. Zhong, and E. Haratsch, "Quasi-cyclic LDPC codes for the magnetic recording channel: code design and VLSI implementation," *IEEE Trans. Magn.*, vol. 43, no. 3, pp. 1118 - 1123 , Mar. 2007.

[8] A. Risso, "Layered LDPC decoding over GF(q) for magnetic recording channel," *IEEE Trans. Magn.*, vol. 45, no. 10, pp. 3683 - 3686 , Oct. 2009.

[9] L. Dolecek, Z. Zhang, V. Anantharam, M. Wainwright, and B. Nikolic, "Analysis of absorbing sets and fully absorbing sets of array-based LDPC codes," *IEEE Trans. Inform. Theory*, vol. 56, no. 1, pp. 181 - 201, Jan. 2010.

[10] B. Amiri, J. Kliewer, and L. Dolecek, "Analysis and enumeration of absorbing sets for non-binary graph-based codes," *IEEE Trans. Commun.*, vol. 62, no. 2, pp. 398 - 409, Feb. 2014.

[11] B. Zhou, J. Kang, Y. Tai, S. Lin, and Z. Ding, "High performance non-binary quasi-cyclic LDPC codes on Euclidean geometries," in *IEEE Trans. Commun.*, vol. 57, no. 5, pp. 1298 - 1311, May 2009.

[12] T. Souvignier, M. Öberg, P. Siegel, R. Swanson, and J. Wolf, "Turbo decoding for partial response channels," in *IEEE Trans. Commun.*, vol. 48, no. 8, pp. 1297 - 1308, Aug. 2000.

[13] D. Declercq and M. Fossorier,, "Decoding algorithms for nonbinary LDPC codes over GF(q)," in *IEEE Trans. Commun.*, vol. 55, no. 4, pp. 633 - 643, Apr. 2007.

[14] B. Amiri, C. Lin, and L. Dolecek, "Asymptotic distribution of absorbing sets and fully absorbing sets for regular sparse code ensembles," in *IEEE Trans. Commun.*, vol. 61, no. 2, pp. 455 - 464, Feb. 2013.